

R-phenyldicarboxyl (R = H, NO₂ and COOH) modular effect on Ni(II) coordination polymers incorporated with a versatile connector 1H-3-(3-pyridyl)-5-(4-pyridyl)-1,2,4-triazole

Bing Li, San-Ping Chen*, Qi Yang, Sheng-Li Gao*

Key Laboratory of Synthetic and Natural Functional Molecule Chemistry of Ministry of Education, College of Chemistry and Materials Science, Northwest University, Xi'an 710069, PR China

ARTICLE INFO

Article history:

Received 3 December 2010

Accepted 13 January 2011

Available online 24 February 2011

Keywords:

3,4'-Hbpt

Benzenedicarboxylate ligand

Ni(II) coordination compound

ABSTRACT

Based on the versatile ligand 1H-3-(3-pyridyl)-5-(4-pyridyl)-1,2,4-triazole (3,4'-Hbpt) (**1**), a series of coordination compounds [Ni(3,4'-Hbpt)(ip)] (**2**), [Ni(3,4'-Hbpt)₂(tp)(H₂O)₂] (**3**), [Ni₂(3,4'-Hbpt)(5-NO₂-ip)₂(H₂O)₄] (**4**) and [Ni(3,4'-Hbpt)(pm)_{0.5}(H₂O)₃]·2H₂O (**5**) have been hydrothermally constructed through R-phenyldicarboxyl (R = H, NO₂ and COOH) intervention effect (ip = isophthalic anion, tp = terephthalic anion, 5-NO₂-ip = 5-NO₂-isophthalic anion, pm = pyromellitic anion). Structural analysis reveals that 3,4'-Hbpt adopts μ-N_{py}, N_{py} coordination modes in two typical conformations in these target coordination compounds. In cooperation with the auxiliary ligands benzenedicarboxylate connectors, a variety of Ni(II) coordination networks such as 2-D layer with (4, 4) topology (**2**) 1-D chain (**3**), honeycomb (**4**) and 2-D helical chains (**5**) have been assembled. Theoretical calculation based on density functional theory (DFT) for ligand (**1**) is also employed to explicate the stability of the different conformations. Moreover, thermal stability of these crystalline materials is explored by TG-DTG.

© 2011 Elsevier Ltd. All rights reserved.

1. Introduction

Currently, extensive experimental and theoretical efforts have been devoted to crystal engineering of coordination polymers from pre-designed bridging ligands and metal ions, because such hybrid materials display a variety of regulated architectures and thus many potential functions [1–8]. Through introducing 1,2,4-triazole between the 3-pyridyl and 4-pyridyl groups, the ligand 1H-3-(3-pyridyl)-5-(4-pyridyl)-1,2,4-triazole (3,4'-Hbpt) has been investigated as a type of excellent rod-like connector to engender a wide range of coordination frameworks [9–12]. What's more, 3,4'-Hbpt has potential tendency to show two typical conformations under appropriate surroundings (Scheme 1). Polycarboxylate species such as isophthalic acid (H₂ip), terephthalic acid (H₂tp), 5-NO₂-isophthalic acid (5-NO₂-H₂ip) and pyromellitic acid (H₄pm) have been extensively explored to produce robust crystalline materials due to their exclusive and versatile coordination ability [13–17]. With this understanding, one crucial aim of this work is to explore the influences of the substituted groups (from –H, –NO₂ to –COOH) of phenyldicarboxyl ligands on the structures of the resultant crystalline materials. In our recent research, we have concentrated on the construction of mixed-ligand metal organic frameworks based on

3,4'-Hbpt and polycarboxylate species. We present crystal structures of the ligand and four new Ni(II) coordination polymers, namely [3,4'-Hbpt]·H₂O (**1**), [Ni(3,4'-Hbpt)(ip)] (**2**), [Ni(3,4'-Hbpt)₂(tp)(H₂O)₂] (**3**), [Ni₂(3,4'-Hbpt)(5-NO₂-ip)₂(H₂O)₄] (**4**) and [Ni(3,4'-Hbpt)(pm)_{0.5}(H₂O)₃]·2H₂O (**5**). The compounds have been structurally established by single-crystal X-ray diffraction analysis, and characterized by IR, EA and TG-DTG. In order to illuminate the stability of the ligand within different conformations, a theoretical analysis has been attempted.

2. Experimental

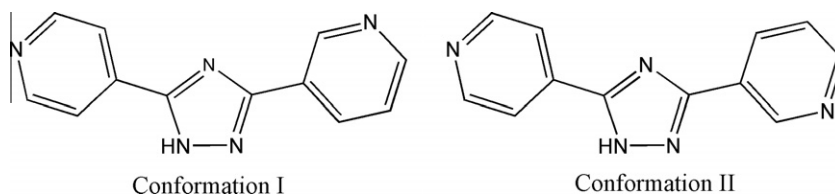
2.1. Materials

Commercially available reagents were used as received without further purification. ¹H NMR spectra were taken with a Varian 400 spectrometer using tetramethylsilane (TMS) as an internal standard. Elemental analyses (C, H and N) were performed on a Vario EL III analyzer. Infrared spectra were obtained from KBr pellets on a BEQ VZNDX 550 FTIR instrument within the 400–4000 cm^{−1} region. Thermogravimetric analysis was carried out on a TA Instruments NETZSCH STA 449C simultaneous TGA with a heating rate of 10 °C min^{−1} under hydrostatic air.

3,4'-Hbpt was synthesized according to the Ref. [18] and further proved by IR and elemental analysis. Anal. Calc. for C₁₂H₉N₅: C,

* Corresponding authors.

E-mail addresses: sanpingchen@126.com (S.-P. Chen), gaoshli@nwu.edu.cn (S.-L. Gao).



Scheme 1. Two typical conformations of 3,4'-Hbpt.

64.56; H, 4.06; N, 31.37. Found: C, 64.88; H, 4.56; N, 32.88%. Mp: 240–241 °C; IR (cm⁻¹, KBr): 3408(w), 3088(m), 1606(s), 1580(s), 1447(m), 1423(m), 1312(m), 1152(s), 1045(m), 987(m), 832(s), 720(m), 709(m), 578(w); ¹H NMR (400 MHz, DMSO-d₆, δ ppm): 6.951–6.980 (1H, d, *J* = 11.6 Hz), 7.508–7.539 (1H, m, *J* = 12.4 Hz), 7.797–7.810 (2H, d, *J* = 5.2 Hz), 8.220–8.240 (1H, d, *J* = 8.0 Hz), 8.662–8.674 (2H, d, *J* = 4.8 Hz), 9.054 (1H, s); 10.329 (1H, s, triazole-H).

2.2. Synthesis of (1)

3,4'-Hbpt (10 mmol) was dissolved in the mixed solution of H₂O (2 ml) and MeOH (20 ml) and the resulting solution was placed in a silicagel desiccator at room temperature for several weeks to give colorless crystals as product **1**. *Anal. Calc.* for **1** (C₁₂H₁₁N₅O): C, 59.74; H, 4.59; N, 29.03. Found: C, 59.80; H, 4.52; N, 29.15%. IR (cm⁻¹, KBr): 3337(s), 3080(s), 3014(s), 1684(m), 1655(s), 1529(s), 1540(s), 1431(s), 1303(m), 1159(m), 1044(w), 1026(w), 910(w), 830(m), 711(m), 662(w), 570(w).

2.3. Synthesis of (2)

A mixture containing Ni(OAc)₂·4H₂O (24.8 mg, 0.10 mmol), 3,4'-Hbpt (11.2 mg, 0.05 mmol), H₂ip (16.6 mg, 0.10 mmol) and water (6 ml) was sealed in a 15 ml Teflon-lined stainless steel vessel, which was heated at 140 °C for 3 days and then cooled to room temperature at a rate of 5 °C h⁻¹. Green prism crystals of **2** were collected in a yield of 25% (based on Ni). *Anal. Calc.* for **2** (C₂₀H₁₃N₅NiO₄): C, 53.85; H, 2.93; N, 15.70. Found: C, 53.89; H, 2.98; N, 15.87%. IR (cm⁻¹, KBr): 3419(w), 3099(m), 1624(s), 1581(w), 1532(m), 1489(m), 1454(m), 1383(s), 993(w), 850(m), 808(m), 758(w), 695(w), 545(w).

2.4. Synthesis of (3)

The same synthetic procedure as that for **2** was used except H₂ip was replaced by H₂tp. Green block crystals of **3** were collected in a yield of 30% (based on Ni). *Anal. Calc.* for **3** (C₃₂H₂₆N₁₀NiO₆): C, 54.49; H, 3.72; N, 19.85. Found: C, 54.51; H, 3.77; N, 19.95%. IR (cm⁻¹, KBr): 3435(m), 3091(m), 3023(m), 1621(s), 1571(s), 1425(m), 1366(s), 983(w), 856(w), 845(w), 758(m), 699(m).

2.5. Synthesis of (4)

The same synthetic procedure as that for **2** was used except that H₂ip was replaced by 5-NO₂-H₂ip. Green prismatic crystals of **4** were collected in a yield of 25% (based on Ni). *Anal. Calc.* for **4** (C₂₈H₂₃N₇Ni₂O₁₆): C, 40.47; H, 2.79; N, 11.80. Found: C, 40.54; H, 2.82; N, 11.89%. IR (cm⁻¹, KBr): 3524(m), 3318(m), 1621(s), 1532(s), 1454(s), 1381(m), 1375(s), 1366(s), 1069(w), 737(m), 553(w).

2.6. Synthesis of (5)

A mixture containing Ni(NO₃)₂·6H₂O (29.1 mg, 0.10 mmol), 3,4'-Hbpt (11.2 mg, 0.05 mmol), H₄pm (25.4 mg, 0.10 mmol) and water (6 ml) was sealed in a 15 ml Teflon-lined stainless steel vessel, which was heated at 160 °C for 3 days and then cooled to room temperature at a rate of 5 °C h⁻¹. Green prism crystals of **5** were collected in a yield of 30% (based on Ni). *Anal. Calc.* for **5** (C₁₇H₂₀N₅NiO₉): C, 41.08; H, 4.06; N, 14.09. Found: C, 41.15; H, 4.12; N, 14.20%. IR (cm⁻¹, KBr): 3376(s), 1621(m), 1561(s), 1425(s), 1375(s), 1326(m), 1140(w), 972(m), 845(w), 688(m).

2.7. X-ray crystallography

All diffraction data of complexes were collected on a Bruker/Siemens Smart Apex IICCD diffractometer with graphite monochro-

Table 1
Crystal data and structure refinement details for 1–5.

	1	2	3	4	5
Empirical formula	C ₁₂ H ₁₁ N ₅ O	C ₂₀ H ₁₃ N ₅ NiO ₄	C ₃₂ H ₂₆ N ₁₀ NiO ₆	C ₂₈ H ₂₃ N ₇ Ni ₂ O ₁₆	C ₁₇ H ₂₀ N ₅ NiO ₉
Formula weight	241.26	446.06	705.34	830.95	497.09
Crystal system	orthorhombic	triclinic	triclinic	triclinic	monoclinic
Space group	<i>Pccn</i>	<i>P</i> $\bar{1}$	<i>P</i> $\bar{1}$	<i>P</i> $\bar{1}$	<i>P2</i> ₁ / <i>n</i>
<i>a</i> (Å)	13.2508(16)	8.7640(13)	8.3890(16)	11.2646(12)	7.3216(10)
<i>b</i> (Å)	15.2685(18)	10.0391(15)	9.4214(19)	11.9753(12)	19.394(3)
<i>c</i> (Å)	11.3208(14)	11.6049(17)	10.669(2)	12.6970(13)	13.9235(18)
α (°)	90	89.360(2)	90.662(2)	113.1820(10)	90
β (°)	90	84.394(2)	108.303(2)	90.9640(10)	97.519(2)
γ (°)	90	67.727(2)	103.312(2)	102.4020(10)	90
<i>V</i> (Å ³)	2290.4(5)	940.0(2)	775.8(3)	1527.9(3)	1960.1(5)
<i>Z</i>	8	2	1	2	4
μ (mm ⁻¹)	0.096	1.072	0.689	1.326	1.055
Unique reflections	2009	3288	2714	6623	3940
Observed reflections	10588	4725	3937	9117	9762
<i>R</i> _{int}	0.0358	0.0210	0.0206	0.0182	0.0558
Final <i>R</i> indices [<i>I</i> > 2σ(<i>I</i>)]	<i>R</i> ₁ = 0.0406, <i>wR</i> ₂ = 0.0592	<i>R</i> ₁ = 0.0388, <i>wR</i> ₂ = 0.0901	<i>R</i> ₁ = 0.0429, <i>wR</i> ₂ = 0.0957	<i>R</i> ₁ = 0.0341, <i>wR</i> ₂ = 0.0837	<i>R</i> ₁ = 0.0548, <i>wR</i> ₂ = 0.1165
<i>R</i> indices (all data)	<i>R</i> ₁ = 0.0636, <i>wR</i> ₂ = 0.0629	<i>R</i> ₁ = 0.0515, <i>wR</i> ₂ = 0.0982	<i>R</i> ₁ = 0.0561, <i>wR</i> ₂ = 0.1043	<i>R</i> ₁ = 0.0434, <i>wR</i> ₂ = 0.0889	<i>R</i> ₁ = 0.0850, <i>wR</i> ₂ = 0.1382

mated Mo K α radiation ($k = 0.71073 \text{ \AA}$) at 293(2) K. Cell parameters were retrieved using SMART [19] software and refined using SAINTPLUS [20,21] for all observed reflections. Data reduction and correction for Lp and decay were performed using the SAINTPLUS software. Absorption corrections were applied using SADABS [22]. All structures were solved by the direct methods using the SHELXS program of the SHELXTL-97 package and refined with SHELXL. Crystallographic details are summarized in Table 1. Selected bond lengths and angles of the complexes are shown in Table S1 (Supplementary material). Possible hydrogen bond geometries of partial complexes are listed in Table S2 (Supplementary material).

3. Results and discussion

3.1. [3,4'-Hbpt]-H₂O (1)

Single crystal X-ray analysis reveals **1** consists of a discrete 3,4'-Hbpt molecule and one lattice water (Fig. 1a). 3,4'-Hbpt adopts conformation I and the dihedral angles between the two pyridine



Fig. 1a. Coordination environment of **1** (lattice water and H atoms are omitted for clarity).

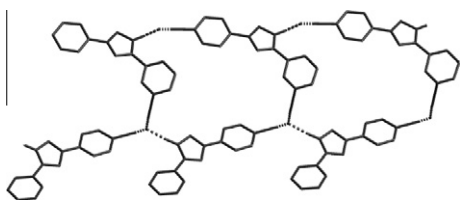


Fig. 1b. Supramolecular structure assembled by hydrogen bonds of the free water molecules.

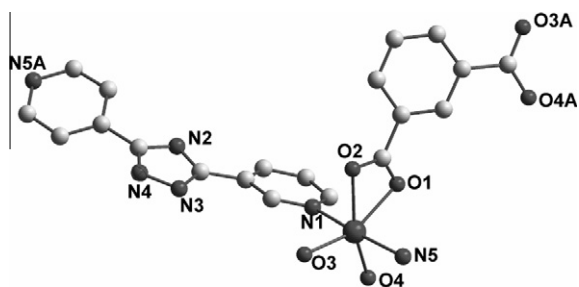


Fig. 2a. Coordination environment of Ni²⁺ in **2** (lattice water and H atoms are omitted for clarity).

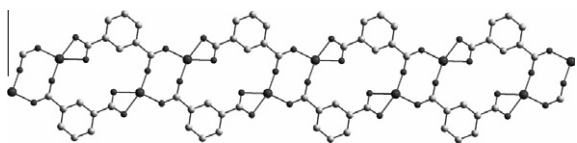


Fig. 2b. The ip-bridged ring-like chain structure.

planes and triazole are 11.98° and 20.23°, respectively. All of these molecules are linked together through weak hydrogen bond interactions such as N3–H3···O1 ($x, -y + 1/2, z + 1/2$), O1–H1W···N (1) ($x, -y + 1/2, z + 1/2$) and O1–H2W···N (5) ($-x, -y + 1, -z + 1$) to form a supramolecular architecture (Fig. 1b).

3.2. [Ni(3,4'-Hbpt)(ip)] (2)

X-ray analysis has revealed that the **2** displays an interesting 2-D layered framework. As shown in Fig. 2a, each nickel ion exhibits a distorted octahedral coordination environment, coordinated by four oxygen atoms from three independent carboxylate groups which are in the equatorial positions and two nitrogen atoms from two 3,4'-Hbpt ligands which locate at the axial positions. Interestingly, 3,4'-Hbpt adopts the conformation II in **2**. The Ni–O_(carboxylate) and Ni–N_(bipy) bond lengths are in agreement with those in carboxylate- and bipy-containing Ni(II) complexes [23]. Each ip²⁻ anion acts as a tetradentate ligand in **2**, connecting three Ni(II) ions. Two carboxylic groups of the H₂ip ligand have different coordination modes, one bidentately bridging two Ni(II) ions in a *syn-syn*

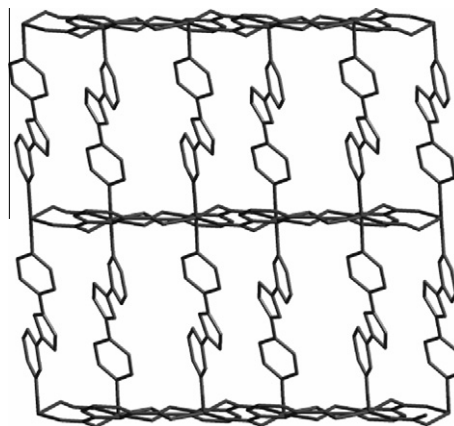


Fig. 2c. The 2-D double-layered framework of **2**.



Fig. 3a. Coordination environment of Ni²⁺ in **3** (lattice water and H atoms are omitted for clarity).

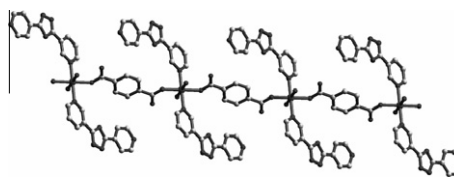


Fig. 3b. The 1-D chain in **3**.

fashion and the other chelating one Ni(II) ion. Along the (0 1 0) direction, the Ni(II) ions are bridged by the ip^{2-} anions to generate 1-D ribbon-like chains containing an alternative arrangement of 8- and 16-membered rings (Fig. 2b). Two carboxylic groups bridge two Ni(II) ions to form an 8-membered ring, and two H_2ip ligands bridge two Ni(II) ions to form a 16-membered ring. The resulting chains are linked by 3,4'-Hbpt to form a 2-D layer (Fig. 2c). The 3,4'-Hbpt twists with a dihedral angle of 34.14° between two pyridine rings planes. From the viewpoint of network topology, we take the adjacent Ni(II) ions as one node, then compound **2** can be simplified as a (4, 4) network.

3.3. $[Ni(3,4'\text{-Hbpt})_2(tp)(H_2O)_2]$ (**3**)

Compound **3** has a 1-D polymeric coordination chain structure. The Ni(II) is coordinated by two carboxylate O atoms from two tp^{2-} ions, two N atoms from two 3,4'-Hbpt ligands and two water molecules (Fig. 3a and 3b). The geometry around the metal center is a slightly distorted octahedron. The tp^{2-} spacers bridge adjacent Ni(II) ions with the Ni...Ni separation of 11.3132(16) Å, leading to a 1-D chain along (1 0 1) direction. Both of the carboxylic groups in the tp^{2-} ligand in **3** adopt monodentate modes to connect with

two Ni atoms, and the 3,4'-Hbpt ligand are in N_{py} coordination fashions.

3.4. $[Ni_2(3,4'\text{-Hbpt})(5\text{-NO}_2\text{-H}_2ip)_2(H_2O)_4]$ (**4**)

Interestingly, with a slight change from H_2ip to 5- NO_2 - H_2ip , a honeycomb net is generated upon reaction with the same metal salt. The asymmetric unit of **4** consists of two Ni(II) cations, one 3,4'-Hbpt molecule, two 5- NO_2 - H_2ip anions, and four coordinated water molecules. Both crystallographically independent Ni(II) ions display a similar octahedral environment, which coordinate with one pyridyl N donors, three carboxylate O atoms, and two water molecules. As shown in Fig. 4a, one carboxylate is monodentate whereas the other exhibits chelating. As a consequence, the adjacent Ni(II) ions are bridged by two 5- NO_2 - H_2ip ligands and one 3,4'-Hbpt ligand to generate a honeycomb net (Fig. 4b).

3.5. $[Ni(3,4'\text{-Hbpt})(pm)_{0.5}(H_2O)_3]\cdot 2H_2O$ (**5**)

Single crystal X-ray analysis indicates **5** features a 2-D coordination polymer. The Ni(II) ion is six-coordinated in the shape of slightly distorted octahedral coordination geometry by one carboxylate oxygen atoms from H_4pm , two pyridyl nitrogen atoms, and three aqua oxygen atoms (Fig. 5a). The Ni–O bond distances range from 2.055(3) to 2.119(3) Å, while the Ni–N bond length is 2.097(4) Å. The pm^{4-} ion acts as a bridge in linking adjacent metal ions through its *para*-positioned carboxylate groups, resulting in

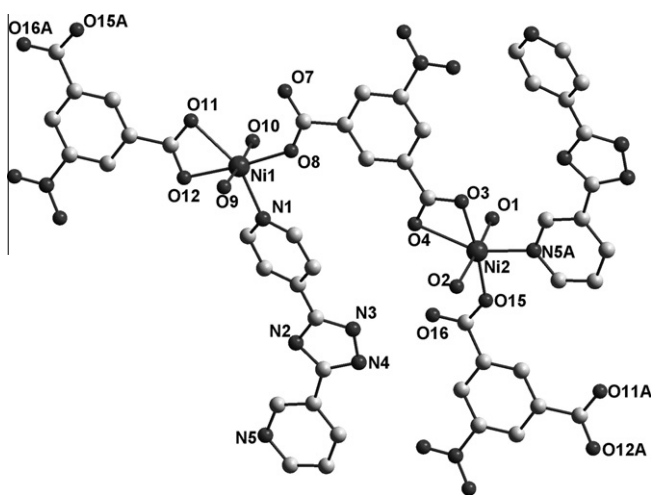


Fig. 4a. Coordination environment of Ni^{2+} in **4** (lattice water and H atoms are omitted for clarity).

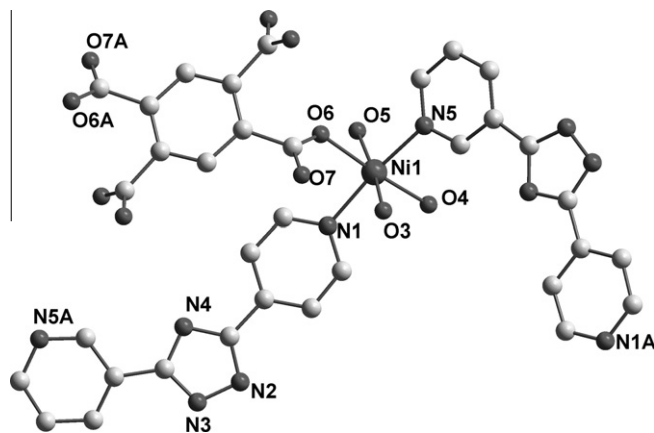


Fig. 5a. Coordination environment of Ni^{2+} in **5** (lattice water and H atoms are omitted for clarity).

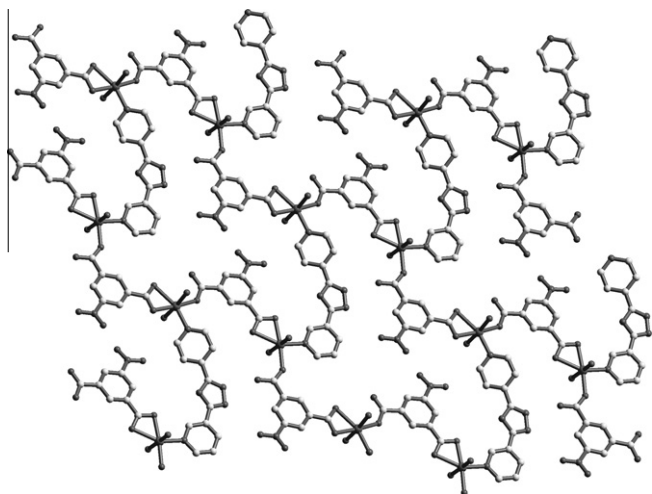


Fig. 4b. The 2-D honeycomb of **4**.

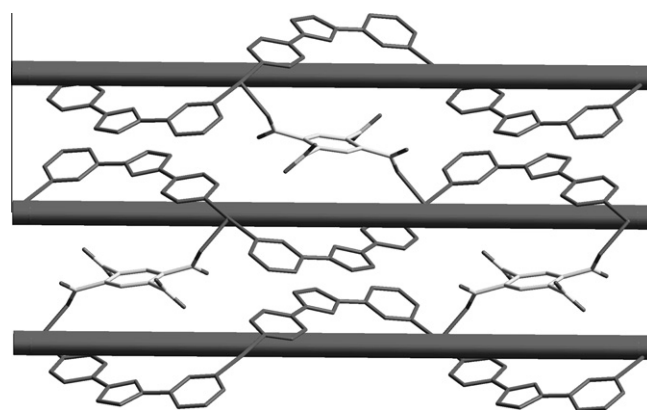


Fig. 5b. The 2-D architecture assembled by right- and left-handed helical chains.

the coordination polymer. The whole structure study on the complex demonstrates that the adjacent Ni(II) ions are linked together through N atoms from 3,4'-Hbpt, forming a metal helical chain. Interestingly, such chains exhibit both right- and left-handed fashions and are connected with carboxylate groups to form an inerratic 2-D architecture (Fig. 5b).

3.6. Quantum chemical calculation of the ligand

In order to further explain stability of the ligand, density functional theory (DFT) calculations have been performed. The structure optimization is performed by means of B3LYP [24,25] with basis sets 6-31G(d). The following calculation and discussion are based on the optimized structure. The full geometry optimization is performed without constraints on symmetry. All computations are carried out with GAUSSIAN 03 quantum chemistry program-package [26].

In the optimized structure, as reported in Table 2, the results of two typical conformations obtained from the basis sets of 6-31G(d) are in conformity with those observed from X-ray analysis. It is reasonable that calculated metal–ligand distances exceed the experimental values by over 0.01 nm [27]. In our case 6-31G(d) gives satisfying results, which differs from the observed parameters only by an average of 0.001 nm, emphasizing a good choice of the level of theory, so the following discussions are based on this result. The energies are -736.448021 and -736.4479373 a.u. for conformation I and conformation II, respectively. Obviously, the conformation I is more stable. What's more, the charges of the N(1), N(5) atoms of the ligand are -0.401 and -0.416 , respectively, indicating N(1) and N(5) are prone to coordination with metal ions.

3.7. Structural diversity and substituent effect and configuration/binding of 3,4'-Hbpt

Structural diversifications are evidently observed in the present series of mixed-ligand coordination compounds. This could be ascribed to the choice of organic ligands since most of them were synthesized under similar reaction conditions. As stated above, one dominating purpose of this research is to elucidate the effects of the substituted groups (from $-H$, $-NO_2$ to $-COOH$) of phenyldicarboxyl ligands on the structures. On the one hand, the nitro group is seldom engaged in coordination with metal ions in this work. As a strong electron withdrawing group [28], however, it will significantly impose on the electronic density of the whole ligand. It can not only behave as a reliable hydrogen-bonding acceptor, but also show the spatial effect. On the other hand, pyromellitic acid may present as the tetranion, trianion, dianion, or monoanion under different conditions, which will greatly affect the assemblies of such supramolecular solids [29–32]. For example, the dideprotonated nature of H_2pm^{2-} acts as a bridge to connect metal ions in this case and also balances the charge of the Ni(II) in the coordination unit. As a matter of fact, we can clearly discover the structural changes (*vide supra*) from **2** (2-D (4, 4) layer) to **4** (2-D honeycomb), as well as from **3** (1-D chain) to **5** (2-D helical chain). Evidently, the results demonstrate that diversity of such coordination polymers can be well regulated by the nature of the phenyldicarboxylate ligands with different substituent groups.

Notably, the structural discrepancy is practically achieved through the versatility of the 3,4'-Hbpt co-ligand in the construction of these coordination arrays. As stated above, the 3,4'-Hbpt molecule may exhibit two typical configurations, both of which have been observed in this work. The conformation I has less steric hindrance effect and always emerges except in the case of **2**, and the $\mu-N_{py}$, N_{py} coordination modes are usually observed in such structures due to different degree of deprotonation.

In summary, we can reveal that for coordination polymers presented herein, the deprotonated polycarboxylate species usually compensate for the charges of divalent metal ions and also link them to form 1-D arrays (ribbon in **2** and single chains in others). Thus, the versatility of the 3,4'-Hbpt will be principally responsible for their structural diversity, for example, the 3,4'-Hbpt connectors in N_{py} coordination fashion are inclined to afford 1-D chain, whereas $\mu-N_{py}$ coordination mode prefer the production of 2-D coordination networks.

Notably, the structural discrepancy is practically achieved through the versatility of the 3,4'-Hbpt co-ligand in the construction of these coordination arrays. As stated above, the 3,4'-Hbpt molecule may exhibit two typical configurations, both of which have been observed in this work. The conformation I has less steric hindrance effect and always emerges except in the case of **2**, and the $\mu-N_{py}$, N_{py} coordination modes are usually observed in such structures due to different degree of deprotonation.

3.8. Thermal stability

The coordination polymers **1**, **3**, **4** and **5** show similar thermal behaviors. They release all water molecules (lattice water for **1**, coordination water for **3** and **4**, both lattice and coordination water for **5**) in the temperature range of 107–128 °C for **1** (found: 6.3%, calcd: 7.5%), 233–267 °C for **3** (found: 5.5%, calcd: 5.1%), 199–249 °C for **4** (found: 10.1%, calcd: 8.6%), and 130–193 °C for **5** (found: 14.7%, calcd: 14.4%), meanwhile, the peak positions appear at 113, 252, 218 and 149 °C, respectively. Subsequently, a complicated weight loss occurs in each case (peaking at 404 °C for **1**, 406 °C for **3**, 414 °C for **4**, 383 °C and 194 °C for **5**, respectively) indicates the decomposition of residual component. **3**, **4** and **5** are with a final residue NiO formed (found: 11.7%, calcd: 10.5% for **3**, found: 17.5%, calcd: 17.8% for **4** and found: 15.8%, calcd: 14.8% for **5**, respectively). As for **2**, it undergoes consecutive steps of weight loss (peaks: 299, 341, 362 and 439 °C) from room temperature, which does not stop until 660 °C with the mass loss of 83.75% (calcd: 83.50%), corresponding to complete conversion to NiO characterized by X-ray powder diffraction analysis.

Acknowledgments

We are grateful to financial support from the National Science Foundation of China (Nos. 20771089, 20873100) and the Natural Science Foundation of Shaanxi Province (No. SJ08B09).

Appendix A. Supplementary data

CCDC 796761, 796759, 796756, 796760 and 697557 contains the supplementary crystallographic data for **1**, **2**, **3**, **4** and **5**. These data can be obtained free of charge via <http://www.ccdc.cam.ac.uk/conts/retrieving.html>, or from the Cambridge Crystallographic Data Centre, 12 Union Road, Cambridge CB2 1EZ, UK; fax: (+44) 1223-336-033; or e-mail: deposit@ccdc.cam.ac.uk. Supplementary data associated with this article can be found, in the online version, at doi:10.1016/j.poly.2011.01.038.

Table 2
Experimental and theoretical parameters for the ligand.

	Calc./6-31G(d)	Exp.		Calc./6-31G(d)	Exp.
<i>Bond length</i>					
N5–C12	1.336	1.337	N3–C7	1.358	1.350
N5–C11	1.338	1.332	N2–N3	1.351	1.362
N4–C6	1.365	1.365	N1–C1	1.338	1.330
N4–C7	1.326	1.327	N1–C5	1.340	1.341
N2–C6	1.335	1.332			
<i>Angles</i>					
C11–N5–C12	117.36	116.57	C6–N4–C7	103.95	103.37
C7–N3–N2	110.98	110.16	C6–N3–N2	102.24	102.39
C1–N1–C5	116.80	115.92			

References

- [1] O.M. Yaghi, M. O'Keeffe, N.W. Ockwig, H.K. Chae, M. Eddaoudi, J. Kim, *Nature* 423 (2003) 705.
- [2] N.W. Ockwig, O. Delgado-Friedrichs, M. O'Keeffe, O.M. Yaghi, *Acc. Chem. Res.* 38 (2005) 176.
- [3] J.P. Zhang, Y.Y. Lin, X.C. Huang, X.M. Chen, *J. Am. Chem. Soc.* 127 (2005) 5495.
- [4] B. Moulton, M.J. Zaworotko, *Chem. Rev.* 101 (2001) 1629.
- [5] M. Du, Z.H. Zhang, Y.P. You, X.J. Zhao, *Cryst. Eng. Commun.* 10 (2008) 306.
- [6] P. Amo-Ochoa, O. Castillo, S.S. Alexandre, L. Welte, P.J. de Pablo, M.I. Rodriguez-Tapiador, J. Gomez-Herrero, F. Zamora, *Inorg. Chem.* 48 (2009) 7931.
- [7] X.M. Chen, M.L. Tong, *Acc. Chem. Res.* 40 (2007) 162.
- [8] W.Y. Sun, M. Yoshizawa, T. Kusakawa, M. Fujita, *Curr. Opin. Chem. Biol.* 6 (2002) 757.
- [9] F.P. Huang, J.-L. Tian, W. Gu, X. Liu, S.P. Yan, D.Z. Liao, P. Cheng, *Cryst. Growth Des.* 10 (2010) 1145.
- [10] F.P. Huang, J.L. Tian, W. Gu, S.P. Yan, *Inorg. Chem. Commun.* 13 (2010) 90.
- [11] Y.L. Zhang, T.L. Liu, S.J. Sun, *Acta Crystallogr., Sect. E* 65 (2009) m1590.
- [12] X.F. Xie, S.P. Chen, Z.Q. Xia, S.L. Gao, *Polyhedron* 28 (2009) 679.
- [13] H. Abourahma, B. Moulton, V. Kravtsov, M.J. Zaworotko, *J. Am. Chem. Soc.* 124 (2002) 9990.
- [14] M. Du, X.J. Jiang, X.J. Zhao, *Chem. Commun.* (2005) 5521.
- [15] J.J. Liu, X. He, M. Shao, M.X. Li, *J. Mol. Struct.* 891 (2008) 50.
- [16] L.F. Ma, L.Y. Wang, J.L. Hu, Y.Y. Wang, S.R. Batten, J.G. Wang, *Cryst. Eng. Commun.* 11 (2009) 777.
- [17] D. Cheng, M.A. Khan, R.P. Houser, *Cryst. Growth Des.* 2 (2002) 415.
- [18] E. Browne, *Aust. J. Chem.* 28 (1975) 2543.
- [19] Bruker AXS, SMART, Version 5.0, Bruker AXS, Madison, WI, USA, 1998.
- [20] Bruker AXS, SAINT-PLUS, Version 6.0, Bruker AXS, Madison, WI, USA, 1999.
- [21] R.H. Blessing, *Acta Crystallogr., Sect. A* 51 (1995) 33.
- [22] G.M. Sheldrick, *Acta Crystallogr., Sect. A* 64 (2008) 112.
- [23] M. Du, X.J. Jiang, X.J. Zhao, *Inorg. Chem.* 46 (2007) 3984.
- [24] A.D. Becke, *J. Chem. Phys.* 98 (1993) 1372.
- [25] C.T. Lee, W.T. Yang, R.G. Parr, *Phys. Rev. B* 37 (1988) 785.
- [26] G.W.T.M.J. Frisch, H.B. Schlegel, G.E. Scuseria, M.A. Robb, J.A.M.J.J.R. Cheeseman, T. Vreven, K.N. Kudin, J.C.J.M.M. Burant, S.S. Iyengar, J. Tomasi, V. Barone, B. Mennucci, G.S.M. Cossi, N. Rega, G.A. Petersson, H. Nakatsuji, M.M.E. Hada, K. Toyota, R. Fukuda, J. Hasegawa, M. Ishida, T.Y.H. Nakajima, O. Kitao, H. Nakai, M. Klene, X. Li, J.E.H.P. H. Knox, J.B. Cross, V. Bakken, C. Adamo, J. Jaramillo, R.E.S.R. Gomperts, O. Yazyev, A.J. Austin, R. Cammi, C.J.W.O. Pomelli, P.Y. Ayala, K. Morokuma, G.A. Voth, P.J.J.D. Salvador, V.G. Zakrzewski, S. Dapprich, A.D.M.C.S. Daniels, O. Farkas, D.K. Malick, A.D. Rabuck, K.J.B.F. Raghavachari, J.V. Ortiz, Q. Cui, A.G. Baboul, S.J.C. Clifford, B.B. Stefanov, G. Liu, A. Liashenko, P.I.K. Piskorz, R.L. Martin, D.J. Fox, T. Keith, M.A.A.I.-C.Y.P. Laham, A. Nanayakkara, M. Challacombe, P.M.W. Gill, W.C.B. Johnson, M.W. Wong, C. Gonzalez, J.A. Pople, GAUSSIAN and R.C. 03, Gaussian Inc., Wallingford, CT, 2004, p. 2020.
- [27] I.A. Guzei, K.R. Crozier, K.J. Nelson, J.C. Pinkert, N.J. Schoenfeldt, K.E. Shepardson, R.W. McGaff, *Inorg. Chim. Acta* 359 (2006) 1169.
- [28] X. Li, R. Cao, W. Bi, Y. Wang, Y. Wang, X. Li, Z. Guo, *Cryst. Growth Des.* 5 (2005) 1651.
- [29] D. Sun, R. Cao, Y. Liang, Q. Shi, M. Hong, *J. Chem. Soc., Dalton Trans.* (2002) 1847.
- [30] O. Fabelo, J. Pasan, L. Canadillas-Delgado, F.S. Delgado, C. Yuste, F. Lloret, M. Julve, C. Ruiz-Perez, *Cryst. Eng. Commun.* 11 (2009) 2169.
- [31] R. Diniz, H. deAbreu, W. de Almeida, M. Sansiviero, N. Fernandes, *Eur. J. Inorg. Chem.* (2002) 1115.
- [32] A. Pramanik, M. Bhuyan, R. Choudhury, G. Das, *J. Mol. Struct.* 879 (2008) 88.